

# PREDICTION OF THE CONTACT THERMAL RESISTANCE OF VERTICAL CARBON NANOTUBE ARRAYS

*Bo SHI* \*, *Han ZHANG*<sup>1</sup>, *Jin ZHANG*<sup>2</sup>

Jiangsu Province Key Laboratory of Aerospace Power System, College of Energy and Power Engineering, Nanjing University of Aeronautics and Astronautics, Nanjing, 210016, CHINA

\* Corresponding author, E-mail: boshi@nuaa.edu.cn

*The Vertical carbon nanotube arrays (VACNTs), as a result of its flexibility and axial high thermal conductivity, exert a huge potential and play an increasingly important role in thermal interface materials (TIMs). This paper proposed a model which can predict the contact thermal resistance of VACNTs. The contact thermal resistance of VACNTs under different pressures is calculated and compared with the experimental data. Also, the effect of variations in the surface roughness and VACNTs parameters on the contact thermal resistance is investigated. Results show that the theoretical results are in good agreement with the experimental data. The contact thermal resistance is composed of interfacial thermal resistance, constriction thermal resistance, and VACNTs resistance. Among which the interfacial thermal resistance is the major thermal resistance. The variations in VACNTs-length and diameter can change the bending degree of VACNTs under the same pressure, which presents important implications on contact thermal resistance and can be used to optimize the contact thermal resistance of VACNTs. The surface roughness exerts little effect on contact thermal resistance.*

*Key words: Vertical carbon nanotube arrays, contact thermal resistance, surface roughness, VACNTs parameters, interfacial thermal resistance*

## 1. Introduction

As early as 2000, Intel Corporation announced that the chip dissipation problem of the personal computer has restricted its power to further improvement [1]. The traditional heat dissipation technique is to transfer the chip heat directly or through the vapor chamber to a heat sink with strong heat dissipation capability. However, the chip and heat sink are mainly connected by solid-solid contact method. The roughness makes the actual contact area small and introduces the contact thermal resistance, which becomes critical in high heat flux.

The use of TIMs is a most effective method to reduce the thermal resistance between two contact interfaces. However, the commonly used TIMs, such as thermal grease, thermal gasket and phase change materials, has a very low effective thermal conductivity. More seriously, the life and reliability of electronic devices will be seriously affected by its problems of aging, failure and leakage. CNTs, ever since it was proved to have high thermal conductivity and strong thermal stability, is the best candidate for adapting to the increasing power of electronics, and can be used to improve the property of TIMs [2-4].

Many scholars have conducted a series of studies on its performance[5-7]. Wang et al. [8] fabricated a bilayer aligned CNT-TIMs and found that it **could** effectively reduce the overall thermal resistance of the TIMs to 8.78 [ $\text{mm}^2 \text{ K/W}$ ]. Khanh et al. [9] measured the thermal resistances of VACNTs using two polymers and found that the reactive polymers, which **was** able to establish covalent bonds with the CNTs, **could** greatly reduce the thermal resistance. Xu et al. [10] found that the addition of the CNT arrays as TIMs **could** reduce the resistance under moderate load compared to the indium sheet and phase-change TIMs, with a minimum resistance of 19.8 [ $\text{mm}^2 \text{ K/W}$ ] at a pressure of 0.445 MPa. Li et al. [11] found that the contact resistance of CNT/polymer **was** lower compared to the CNT/metal. Hirotani et al [12] measured the interfacial thermal resistance (ITR) between the VACNTs and SiO<sub>2</sub> surface and found that the ITR between the VACNTs tip and the SiO<sub>2</sub> surface **was** independent of contact pressure. **To improve the in-plane thermal conduction of VACNT arrays, Kong et al. [13] proposed a three dimensional CNT network structure and found that the in-plane thermal conductivity is  $5.40 \pm 0.92 \text{ W/m}^1\text{K}^{-1}$ , nearly 30 times higher than the VACNT arrays. Kaur et al. [14] connected the metal surfaces and VACNTs with short, covalently bonded organic molecules to enhance thermal transport at the interface and showed a sixfold reduction in the thermal interface resistance. Sun et al. [15] also experimentally demonstrated that it can improve thermal transport between the VACNTs and graphene hybrid material interfaces by Covalent Bonds.**

The above researches on the performance of VACNTs are experimental oriented. Based on the experimental results and mathematical analysis, many scholars proposed a number of models and assumptions to calculate the contact thermal resistance and began to carry out theoretical research. Hu et al. [16] studied the effects of the crossing angle, nanotube length and initial nanotube spacing on the thermal resistance of the crossed CNTs by the nonequilibrium molecular dynamics (MD) method, founding that the thermal resistance increases with the increase of crossing angle and initial nanotube spacing, while decreases with the increasing nanotube length. Yovanovich et al. [17] proposed a CMY plastic contact thermal resistance model, which **indicated** that the surface asperities are satisfied with the Gaussian distribution. **By comparing the surface asperities with the particles in statistical thermodynamics,** Leung et al. [18] studied the contact thermal resistance and its interaction mechanism. However, there is few satisfactory theoretical model to predict the thermal resistance of various conditions, and the empirical formula for describing the effects of various factors such as VACNTs parameters and surface roughness on contact thermal resistance is still unclear.

In this paper, a model which can predict the thermal contact resistance of the VACNTs is proposed. It presents a complete description from contact analysis to the calculation of the contact thermal resistance. The theoretical results are compared with the experimental date. Also, the effect of variations in the surface roughness and CNTs parameters on the contact thermal resistance is studied particularly, with the aim of obtaining some useful information for optimizing the contact thermal resistance of VACNTs.

## 2. Model description

The contact of two rough surfaces can be simplified to the contact between a randomly rough surface and a rigid smooth surface [19]. As shown in fig. 1, a rough copper surface is contact with a smooth Si surface which is grown with VACNTs on it. Without VACNTs, incomplete contact between two surfaces caused by the roughness of the copper surface will lead to the heat flow contraction, resulting in high contact thermal resistance. While the VACNTs are deposited on it, the

contact area is greatly enhanced due to the flexibility of VACNTs, and at the same time, the contact thermal resistance is greatly reduced.

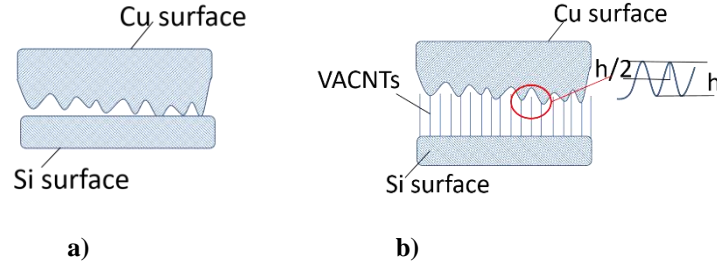


Figure 1. Contact between a) Cu surface and Si surface, and b) VACNTs as TIMs

## 2.1. Mechanical analysis of CNTs

Many scholars have studied the mechanical properties of CNTs and indicated that the macroscopic mechanical model could be applied to calculate its mechanical properties [20, 21]. In this paper, the CNT is considered as a elastic rod with initial curvature. The force diagram of the rod is shown in fig. 2. Liu et al. [22] deduced the flexible line equation of the compressed straight rod in Cartesian coordinate system, which is derived from the curve coordinates. And it is applied to calculate the force of the CNTs.

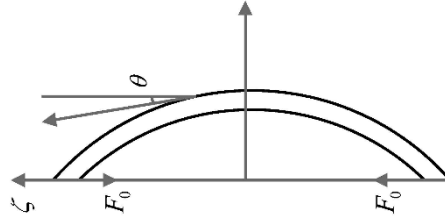


Figure 2. The force diagram of a rod

Force of the CNTs is calculated as:

$$F_0 = 4EI / L^2 \left( \int_0^{\pi/2} \frac{d\varphi}{\sqrt{1-k^2 \sin^2 \varphi}} \right) \quad (1)$$

where  $\sin \varphi = \sin \frac{\theta}{2} / k$ ,  $k = \sin \frac{\theta_0}{2}$  and  $E = 1$ ,  $F_0$  is the force of the CNTs with initial curvature,  $E$  is the Young's modulus of CNTs.

Axial displacement of the CNTs is calculated as:

$$\xi(\varphi) = \frac{L}{2 \int_0^{\pi/2} \frac{d\varphi}{\sqrt{1-k^2 \sin^2 \varphi}}} \left( \int_0^{\varphi} \frac{1-2k^2 \sin^2 \varphi}{\sqrt{1-k^2 \sin^2 \varphi}} d\varphi \right) \quad (2)$$

Eqs. (1) and (2) include an elliptic integral, which makes it difficult to calculate the analytical solution. In this paper, the numerical solution is applied to find the results of the eqs. (1) and (2).

## 2.2. Analysis of surface roughness

In the contact process, the actual contact occurs only on a small number of discrete asperities due to the influence of roughness. Studies show that the asperity distribution of most rough surfaces is random and close to Gaussian distribution, and the deformation of asperity in the process of contact can be considered to be elastic [23, 24]. The effect of roughness on the contact resistance of VACNTs

is considered in this model as well, which is described by Greenwood and Williamson's model (GW). The GW model uses a parabolic function to describe the peak. The peak height on the midpoint is corresponding to the Gaussian distribution [25]:

$$\phi(z) = \frac{1}{\sqrt{2\pi}\sigma} \exp\left(-\frac{z^2}{2\sigma^2}\right) \quad (3)$$

Where  $\sigma = \sigma_1^2 + \sigma_2^2$  is the equivalent roughness of the contact surfaces.

When the Si surface is in direct contacted with the copper surface, the contact area between them is much smaller than the nominal contact area and the peak parts are the major influencing factors. While the VACNTs are used as the TIMs, the contact area in the valley parts becomes larger and the valley parts should be considered. Therefore, a convex model is proposed in our work, assuming that the peak height is constant. The shape of the convex is shown in fig. 1(b), the enlarged image in the red circle. When dealing with the contacting surfaces, two reference planes are defined. One is the mean of the asperity heights and the other is the mean of the copper surface heights, as shown in fig. 3.

In the case of contact model analysis, there assumptions are hypothesized as discussed in many articles [26]: 1) The radius of curvature of the asperity is same. 2) The height of the asperity satisfies Gaussian distribution. 3) The contact between the asperities is elastic.

The peak height can be calculated as:

$$h = 1 / 4\pi\rho\eta \quad (4)$$

where  $\rho = \rho_1\rho_2 / (\rho_1 + \rho_2)$  is the equivalent peak curvature.

According to the above assumptions, the shape of the asperities is ultimately determined by three parameters:  $\sigma, \rho$  and  $\eta$ . The deformation of the asperities is neglected in this paper considering that its deformation is much smaller than that of CNTs.

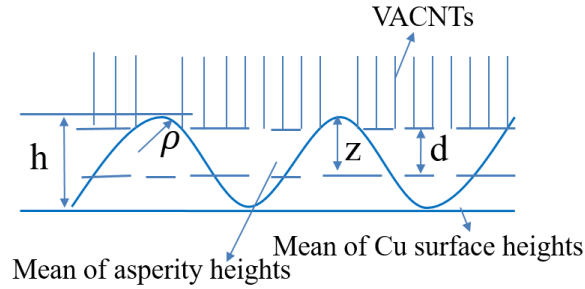


**Figure 3. The basic geometry model of contacting surfaces**

The specific calculation steps of the model are as follows :

The total number of asperities in contact is calculated as:

$$N_c = \eta A_n \int_d^\infty \phi(z) dz \quad (5)$$

Define the normal deformation is:

$$w = z - d \quad (6)$$

During loading, the contact area,  $A_c$ , and the contact force,  $F_c$ , of each individual asperity are only related to the deformation of the asperities,  $w$ , when it is assumed that there is no interference between asperities. That is to say:

$$A_e = A(w), F_e = F(w) \quad (7)$$

Then the total contact area and contact pressure are calculated as:

$$\begin{aligned} A(d) &= \eta A_n \int_d^\infty A_e(z-d)\phi(z)dz \\ P(d) &= \eta \rho_{\text{cnt}} \int_d^\infty F_e(z-d)\phi(z)dz \end{aligned} \quad (8)$$

The function that describes the profile of the peak is a piecewise function, so  $A_e(w)$  and  $F_e(w)$  are also piecewise function and its expression is as follows:

$$\begin{aligned} A_e(w) &= \begin{cases} 2\pi\rho w, (w \leq h/2); \\ (1/\eta - 2\pi\rho h) + 2\pi\rho w, (h/2 < w \leq h); \\ 1/\eta, (w > h), \end{cases} \quad (9) \\ F_e(w) &= \begin{cases} \int_0^{\sqrt{2\pi w/\rho}} (F_0 w - F_0 \rho x^2 / 2) \pi x dx, (w \leq h/2); \\ \int_0^{\sqrt{\pi h/2\rho}} (F_0 w - F_0 \rho x^2 / 2) \pi x dx \\ + \int_{\sqrt{\pi h/2\rho}}^{\sqrt{\pi h/\rho - \sqrt{2(w+d)/\rho}}} (F_0 w - F_0 h + F_0 \rho(x - \sqrt{\pi h/\rho}) / 2) \pi x dx, (h/2 < w \leq h); \\ \int_0^{\sqrt{\pi h/2\rho}} (F_0 w - F_0 \rho x^2 / 2) \pi x dx + \int_{\sqrt{\pi h/2\rho}}^{\sqrt{\pi h/\rho}} (F_0 w - F_0 h + F_0 \rho(x - \sqrt{\pi h/\rho}) / 2) \pi x dx, (w > h). \end{cases} \quad (10) \end{aligned}$$

### 3. Contact resistance calculation

The contact thermal resistance is composed of three mainly parts: the interfacial thermal resistance which is caused by the difference of the phonon spectrum **and the electron spectrum** between the VACNTs and the copper surface, and the constriction thermal resistance which is caused by the incomplete contact, as well as the thermal resistance of CNTs.

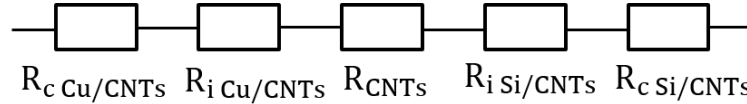


**Figure 4. The thermal resistance network for the model**

The thermal resistance network for the model is shown in fig. 4. The total thermal resistance is:

$$R_{\text{total}} = R_{c \text{ Cu/CNTs}} + R_{i \text{ Cu/CNTs}} + R_{\text{CNTs}} + R_{i \text{ Si/CNTs}} + R_{c \text{ Si/CNTs}} \quad (11)$$

In which,  $R_{c \text{ Cu/CNTs}}$  and  $R_{c \text{ Si/CNTs}}$  are the constriction thermal resistance of Cu-CNTs and Si-CNTs, respectively,  $R_{i \text{ Cu/CNTs}}$  and  $R_{i \text{ Si/CNTs}}$  are the interfacial thermal resistance of Cu-CNTs and Si-CNTs, respectively, and  $R_{\text{CNTs}}$  is the thermal resistance of the VACNTs.

In the calculation of the contact resistance model, assuming that there is no heat loss during contact, all heat flows are transferred by contact between solids and the physical parameters are constant during heat transfer [27].

#### 3.1. Interfacial thermal resistance

Many scholars have used molecular dynamics to study the interface resistance and heat transfer characteristics between CNTs and the target surface, which is also used in this paper.

The Tersoff potential energy is used to describe the interaction between carbon atoms and silicon atoms, as many scholars have done [28, 29]. The Embedded Atom Met (EAM) potential is applied to simulate the interaction between copper atoms [30, 31]. And the LJ potential energy is selected to describe the interaction between copper and carbon atoms in view of the fact that many scholars have adopted van der Waals [32].

The interfacial thermal resistance is composed of the Cu-CNTs interfacial thermal resistance and the Si-CNTs interfacial thermal resistance. As mentioned in the above paragraph, the interaction in carbon atoms and silicon atoms are all the Tersoff potential, which indicates that the silicon and carbon atoms are tightly connected with each other when in direct contact just like the same atoms, **therefore**, the Si-CNTs interfacial thermal resistance can be considered very small, far less than the Si-CNTs interfacial thermal resistance, and can be omitted in calculation.

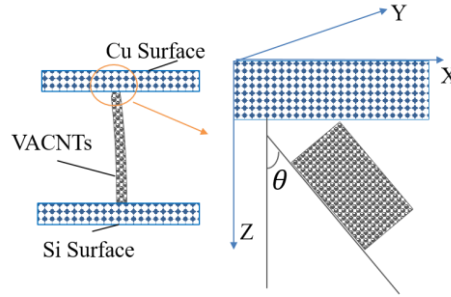


**Figure 5. The interface models in Cu-CNT-Si structure**

The Cu-CNTs interfacial thermal resistance, which is caused by the mismatch of the CNTs and the copper lattice, is calculated by the molecular dynamics. Figure 5 shows the interface models simulated between CNT and copper crystal. The upper part is “ fcc ” copper crystal with bottom surface (001) . The lower part is (10, 10) CNT structure. The contact angle  $\theta$  between the CNT and the copper surface is the angle between the axis of the CNT and the nominal direction of the copper surface. Periodic boundary condition is used in the X and Y directions.

The interfacial thermal resistance of single CNT contacted with copper lattice is [33]:

$$r_i = \Delta T / Q \quad (12)$$

This paper assumes that  $r_i$  is only depended on the contact angle. The interfacial thermal resistance of the whole surface can be calculated as:

$$R_{i \text{ Cu/CNTs}} = A_n \sum_{\theta} [r_i(\theta) / n_i(\theta)] \quad (13)$$

### 3.2. Constriction thermal resistance

The constriction resistance is caused by the constriction of heat flow at the rough contact surface. When the VACNTs are used as the TIMs, the constriction thermal resistance is the sum of the Cu-CNTs constriction thermal resistance and the Si-CNTs constriction thermal resistance. The length of the VACNTs is much smaller compared to the incomplete contact gap between the two contact surfaces, therefore, it can be simplified to the calculation of the constriction thermal resistance in Cu-Si surfaces.

The individual constriction thermal resistance per unit area can be described as [34]:

$$r_c = (1 - a/b)^{1.5} / (2ak_c) \quad (14)$$

where  $a = \sqrt{A(d)/\pi N_c}$ ,  $b = \sqrt{A_n/\pi N_c}$ ,  $k_e = k_1 k_2 / (k_1 + k_2)$  is the equivalent thermal conductivity.

Total constriction resistance can be calculated as:

$$R_c = R_{c_{Cu/CNTs}} + R_{c_{Si/CNTs}} = A_n r_c / N_c \quad (15)$$

### 3.3. Thermal resistance of VACNTs

When the heat goes through the VACNTs, the thermal resistance generated by the heat transfer between the CNTs and the CNT-defects will result in the thermal resistance of CNTs. Previous work show that the thermal conductivity of CNTs varies from hundreds to thousands [ $\text{W/m}^1\text{K}^{-1}$ ]. Eric et al. [35] stated that the thermal conductivity of SWCNTs was close to 3500 [ $\text{W/m}^1\text{K}^{-1}$ ]. Fujii et al. [36] found that when the CNTs-diameter was 16.1nm, the axial thermal conductivity of the CNTs was about 1800 [ $\text{W/m}^1\text{K}^{-1}$ ] at room temperature. Bi et al. [37] concluded that the thermal conductivity of SWCNTs was about 600 [ $\text{W/m}^1\text{K}^{-1}$ ] with the length of the SWCNTs varying from 2.5 to 25nm. They also pointed out that the high thermal conductivity of CNTs was mainly determined by phonon Heat conduction rather than electronic heat conduction.

The thermal resistance of CNTs is described as:

$$R_{CNTs} = (L / k_c A_c) / N \quad (16)$$

The thermal resistance of the CNTs under different thermal conductivity is calculated according to the parameters in tab. 2 and the results are shown in tab. 1.

**Table 1. Thermal resistance of CNTs**

$k_c = 600 [\text{W/m}^1\text{K}^{-1}]$			$k_c = 3500 [\text{W/m}^1\text{K}^{-1}]$		
$P$	$R_{total}$	$R_{CNTs}$	$P$	$R_{total}$	$R_{CNTs}$
0.31	43.77	2.22	0.31	41.93	0.38
0.27	50.56	2.56	0.27	48.45	0.44
0.23	58.78	2.97	0.23	56.32	0.51
0.20	68.75	3.47	0.20	65.88	0.60
0.17	80.93	4.07	0.17	77.55	0.70

When the thermal conductivity of CNTs varies from 600 [ $\text{W/m}^1\text{K}^{-1}$ ] to 3500 [ $\text{W/m}^1\text{K}^{-1}$ ], the thermal resistance of the CNTs has a slight decrease and is much smaller compared to the total thermal resistance. The variations in thermal conductivity of CNTs have little

impact on the total thermal resistance. In this paper, we choose  $k_c = 2000[\text{W/m}^1\text{K}^{-1}]$  as the thermal conductivity of CNTs.

## 4. Results and discussion

According to the above description, a computer program was developed to solve the results numerically. The thermal contact resistance under various pressures is calculated and compared to the experimental results. The influence of the peak curvature, the number of asperities per unit area, the standard deviation of the peak distribution, and the influence of the CNT-length, diameter and density on the thermal resistance are analyzed respectively.

### 4.1. Comparison with experimental data

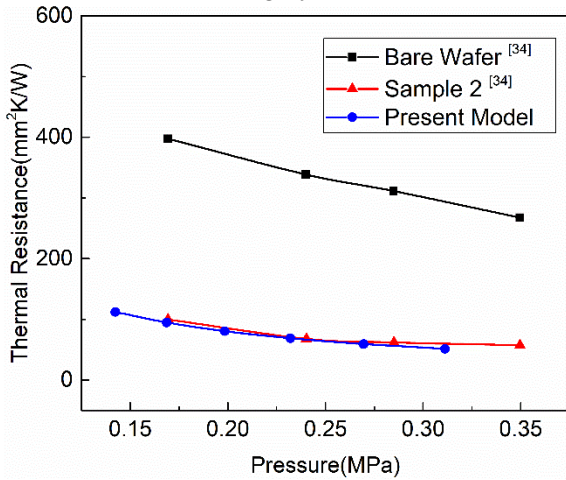
Xu et al. [38] measured the contact thermal resistance between a copper surface and a silicon surface which is grown with CNTs on it. The contact thermal resistance for the uncoated control sample (a sample that without the CNTs as TIMs) is also included for comparison. The surface roughness of Si and Cu are 0.09 and 1 and the thermal conductivities for Cu and Si take constant values of 391.1 [ $\text{W/m}^1\text{K}^{-1}$ ] and 141 [ $\text{W/m}^1\text{K}^{-1}$ ], respectively.

With the above parameters, the equivalent roughness and thermal conductivity can be obtained. The specific calculation parameters needed in this paper are shown in tab. 2. Then the computational procedure was run to construct the results.

**Table 2. Specific calculation parameters**

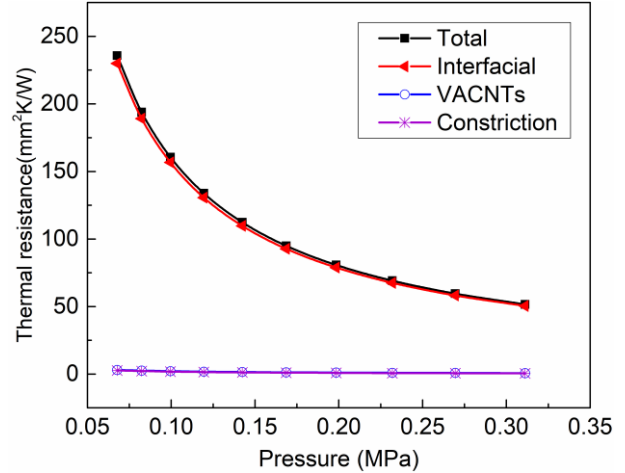
Calculation Parameters			
Parameters of Roughness		Parameters of VACNTs	
$\sigma, [\mu\text{m}]$	1	$D, [\text{nm}]$	50
$\rho, [\mu\text{m}]$	150	$L, [\mu\text{m}]$	12
$\eta, [\text{mm}^2]$	350	$\rho_{\text{cnt}}, [\mu\text{m}^{-2}]$	200
$k_c, [\text{W}/\text{m}^{-1}\text{K}^{-1}]$	104	$k_c, [\text{W}/\text{m}^{-1}\text{K}^{-1}]$	2000

Figure 6 shows the comparative results between the present model and the experimental data of Xu et al. It can be seen that the theoretical results are in good agreement with the experimental data. As the pressure increases, the thermal resistance decreases and tends to be flat. With high-quality VACNTs, the thermal resistance in present model is two to three times lower than the values of the bare wafer (without CNTs between Cu-Si surfaces), which demonstrates that the adoption of the CNTs as TIMs can largely reduce the thermal resistance between the contact surfaces.



**Figure 6. Comparison of present model with experimental data of Xu et al.**

Figure 7 shows the contact thermal resistance of present model as a function of pressure. The graph plots Thermal resistance (mm²K/W) on the y-axis (0 to 250) against Pressure (MPa) on the x-axis (0.05 to 0.35). Four data series are shown: 'Total' (black squares), 'Interfacial' (red triangles), 'VACNTs' (blue circles), and 'Constriction' (purple crosses). The Total and Interfacial series are nearly identical, starting at approximately 230 mm²K/W at 0.05 MPa and decreasing to about 50 mm²K/W at 0.35 MPa. The VACNTs and Constriction series are very low, remaining near 0 mm²K/W across the entire pressure range.



**Figure 7. Contact thermal resistance of present model as a function of pressure**

Figure 7 shows the contact thermal resistance as a function of pressure. The contact thermal resistance composes three thermal resistances: the interfacial thermal resistance, the constriction thermal resistance, as well as the thermal resistance of CNTs. It can be seen that all the three thermal resistances are inversely proportional to the pressure, that is, with the pressure increasing, the three thermal resistances tend to decrease. The effect of constriction resistance and VACNTs resistance on contact resistance can be neglected and the total thermal resistance is determined only by the interfacial thermal resistance. Therefore, the interfacial thermal resistance is the major thermal resistance.

The point contact between the VACNTs tips and the Cu surface results in a decrease in the actual contact area, which is the major cause of the larger interfacial thermal resistance. Applying thermal grease/gels or phase change materials (PCMs) to the interfaces can create more heat flow path between the VACNTs and the target surface, which might significantly reduce the interfacial thermal resistance.

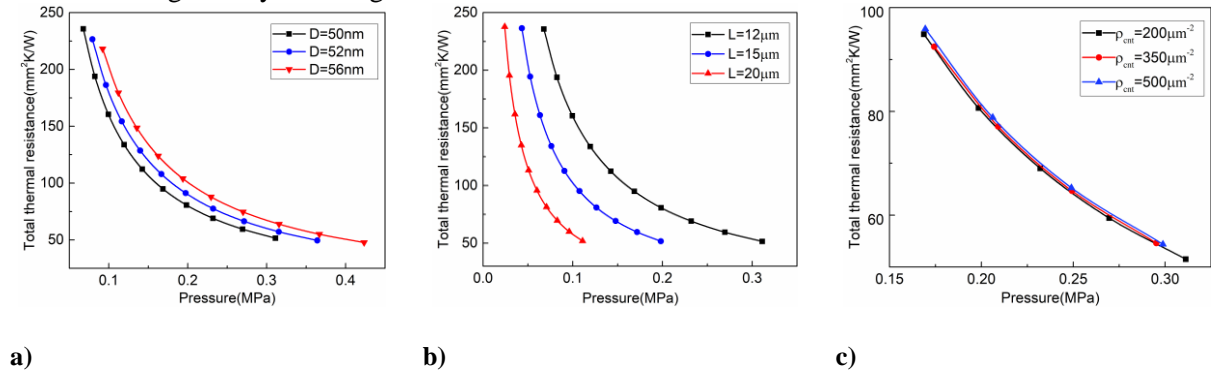
#### 4.2. The influence of the VACNTs parameters on contact thermal resistance

Figure 8 shows the influence of the VACNTs parameters on contact thermal resistance. With the VACNTs-length increased and the VACNTs-diameter declined, the slope of the total thermal



resistance-pressure curve increases, which indicates that the influence of pressure on the total thermal resistance becomes stronger. The increase of the VACNTs-length and the decline of the VACNTs-diameter makes it easier for VACNTs to compress under the same pressure and becomes bent. The bending of the VACNTs increases the heat transfer area between the VACNTs and the copper surface in the whole VACNTs arrays, resulting in the heat conduction channel raised and the total thermal resistance reduced, which can be used to account for the result shown in figs. 8 (a) and (b). When the pressure is from 0.15 MPa to 0.35 MPa, there is a little bit increase in total thermal resistance as the VACNTs-density increases. Because the increase in VACNTs-density makes the point contact between the VACNTs tips and the Cu surface increase, but at the same time, it also makes the VACNTs difficult to compress. The heat transfer area between the VACNTs and the copper surface which is caused by the bending of the VACNTs will decrease, resulting in the heat transfer channel reduced and the total thermal resistance raised.

Therefore, the bending degree of VACNTs has important implications on the total thermal resistance. As the bending degree enhanced, the total thermal resistance will decrease gradually. When the VACNTs-density is determined, the contact thermal resistance can be reduced by increasing the VACNTs-length or by reducing the VACNTs-diameter.



**Figure 8. The influence of a) the VACNTs- diameter, b) the VACNTs-length and c) the VACNTs-density on contact thermal resistance**

### 4.3. The influence of the roughness on contact thermal resistance

As can be seen from the analysis of surface roughness described by GW model in Section [2.2], the roughness is mainly determined by the standard deviation of the peak distribution and the peak height which is subject to the peak curvature and the number of asperities per unit area. The influence of these three factors on the roughness is shown in fig. 9. Figure 9 (a) and (b) illustrate the influence of the peak height on contact thermal resistance. With the increase of the peak curvature and the number of asperities per unit area, the total thermal resistance is almost unchanged, indicating that the peak height, that is, the shape of the peaks has little effect on total thermal resistance.

The determining factor affecting roughness is the standard deviation of the peak distribution. As it increases, the total thermal resistance exhibits a slight increase, as shown in fig. 9 (c). With the standard deviation of the Gaussian distribution increasing, the copper surface gets rougher. When it is subject to different pressures, the contact area between the copper surface and the VACNTs will decrease, resulting in a reduction in the heat conduction channels and a slight raise in total thermal resistance. From the above analysis, we can draw the conclusion that the surface roughness exerts little effect on the total contact thermal resistance.

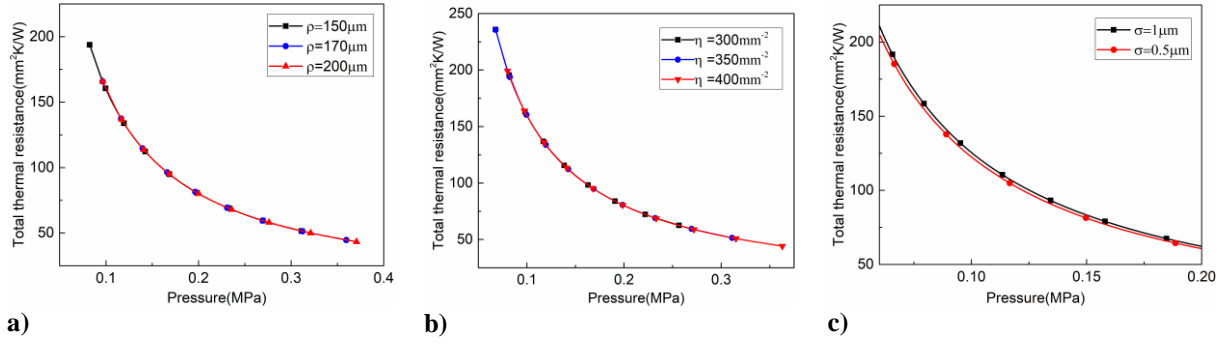


**Figure 9. The influence of a) the peak curvature, b) the number of asperities per unit area and c) the standard deviation of the peak distribution on contact thermal resistance**

## 5. Conclusions

A model is proposed in this paper to calculate the thermal contact resistance of VACNTs, which is composed of interfacial thermal resistance, constriction thermal resistance, and VACNTs resistance. The theoretical results are in good agreement with the experimental data. With the high-quality VACNTs, the total thermal resistance in present model is two to three times lower than the values of the bare wafer (without CNTs between Cu-Si surfaces) and the interfacial thermal resistance is the major thermal resistance. The bending degree of VACNTs has important implications on the total thermal resistance. As the bending degree enhanced, the total thermal resistance will decrease gradually. When the VACNTs-density is determined, the contact thermal resistance can be reduced by increasing the VACNTs-length or by reducing the VACNTs-diameter. While the surface roughness exerts little effect on contact thermal resistance. By using this calculation model, it can provide more accurate parameters for optimizing the contact thermal resistance of VACNTs.

## Acknowledgement

This research was supported by National Key Basic Research Program of China ( No: 2014CB239603)

## Nomenclature

$A$	-total contact area, [m <sup>2</sup> ]
$A_e$	-contact area of each individual asperity, [m <sup>2</sup> ]
$A_c$	-cross-section of CNTs, [m <sup>2</sup> ]
$A_n$	-nominal contact area, [m <sup>2</sup> ]
$a$	-radius of the contact area, [ $\mu\text{m}$ ]
$b$	-radius of the heat transfer channel, [ $\mu\text{m}$ ]
$D$	-diameter of CNTs, [nm]
$d$	-distance between the CNTs-top and the middle line of peak when CNTs are uncompressed, [ $\mu\text{m}$ ]
$E$	-Young's modulus of CNTs, [TPa]
$F_0$	-external contact force of the CNTs with initial curvature, [N]
$F_e$	-external contact force of each individual asperity, [N]
$h$	-peak height, [ $\mu\text{m}$ ]
$I$	-moment of inertia of the cross-section
$k_c$	-thermal conductivity of CNTs, [W/m <sup>1</sup> K <sup>-1</sup> ]
$k_1, k_2$	-thermal conductivities of Si surface and Cu surface, respectively, [W/m <sup>1</sup> K <sup>-1</sup> ]

$L$	-length of CNTs, [ $\mu\text{m}$ ]
$N$	-number of CNTs per unit area contact with the asperities
$N_c$	-total number of asperities in contact
$n_i$	-number of CNTs with different $\theta$
$P$	-Contact pressure, MPa
$Q$	-heat flux through the interface, [ $\text{mm}^2/\text{W}$ ]
$R_{\text{total}}$	-total thermal resistance, [ $\text{mm}^2\text{K}/\text{W}$ ]
$R_c$	-total constriction resistance= $(R_{c, \text{Cu}/\text{CNTs}} + R_{c, \text{Si}/\text{CNTs}})$ , [ $\text{mm}^2\text{K}/\text{W}$ ]
$R_{\text{CNTs}}$	-thermal resistance of the VACNTs, [ $\text{mm}^2\text{K}/\text{W}$ ]
$R_{i, \text{Cu}/\text{CNTs}}, R_{i, \text{Si}/\text{CNTs}}$	- interfacial thermal resistance of Cu-CNTs and Si-CNTs, respectively, [ $\text{mm}^2\text{K}/\text{W}$ ]
$r_c$	-individual constriction thermal resistance per unit area, [ $\text{mm}^2\text{K}/\text{W}$ ]
$r_i$	-interfacial thermal resistance of single CNTs contacted with copper lattice, [ $\text{mm}^2\text{K}/\text{W}$ ]
$\Delta T$	-temperature difference between the copper lattice and the CNT, [K]
<b>Greek symbols</b>	
$\theta_0, \theta$	-bending angle of the CNTs with initial curvature, and under different force
$\xi$	-axial displacement of the CNTs, [ $\mu\text{m}$ ]
$\sigma_1, \sigma_2$	- roughness of the Si surface and Cu surface, respectively, [ $\mu\text{m}$ ]
$\rho_1, \rho_2$	-peak curvature of the Si surface and Cu surface, respectively, [ $\mu\text{m}$ ]
$\rho_{\text{cnt}}$	-density of the CNTs, [ $\mu\text{m}^{-2}$ ]
$\eta$	-number of asperities per unit area, [ $\text{mm}^{-2}$ ]

## References

- [1] Viswanath, R., *et al.*, Thermal Performance Challenges from Silicon to Systems, *Intel Corporation Tech Rep.* (2000), 3
- [2] Shaikh, S., *et al.*, Thermal Conductivity of an Aligned Carbon Nanotube Array, *Carbon.*, 45. (2007), 13, pp. 2608-2613, DOI No. 10.1016/j.carbon.2007.08.011
- [3] Xie, H., *et al.*, Thermal Diffusivity and Conductivity of Multiwalled Carbon Nanotube Arrays, *Physics Letters A*, 369. (2007), 1–2, pp. 120-123, DOI No. 10.1016/j.physleta.2007.02.079
- [4] Choi, T.Y., *et al.*, Measurement of Thermal Conductivity of Individual Multiwalled Carbon Nanotubes by the 3- $\omega$  Method, *Applied Physics Letters*, 87. (2005), 1, p. 56, DOI No. 10.1063/1.1957118
- [5] Zhang, Y., *et al.*, Compliance Properties Study of Carbon Nanofibres (CNFs) Array as Thermal Interface Material, *Journal of Physics D Applied Physics*, 41. (2008), 15, p. 155105, DOI No. 10.1088/0022-3727/41/15/155105
- [6] Zhang, K., *et al.*, Carbon Nanotube Thermal Interface Material for High-brightness Light-emitting-diode Cooling, *Nanotechnology*, 19. (2008), 21, p. 215706, DOI No. 10.1088/0957-4484/19/21/215706
- [7] Zhang, G., *et al.*, Temperature Dependence of Thermal Boundary Resistances between Multiwalled Carbon Nanotubes and Some Typical Counterpart Materials, *Acs Nano*, 6. (2012), 6, pp. 3057-3062, DOI No. 10.1021/nn204683u
- [8] Wang, H., *et al.*, Reducing Thermal Contact Resistance Using a Bilayer Aligned CNT Thermal Interface Material, *Chemical Engineering Science*, 65. (2010), 3, pp. 1101-1108, DOI No. 10.1016/j.ces.2009.09.064
- [9] Khanh, H.L., *et al.*, Enhancement of the Thermal Properties of a Vertically Aligned Carbon Nanotube Thermal Interface Material Using a Tailored Polymer, *Journal of Applied Heat Transfer*, 11. (2012), 4, pp. 1 - 4
- [10] Xu, J., T.S. Fisher, Enhancement of thermal interface materials with carbon nanotube arrays, *International Journal of Heat & Mass Transfer*, 49. (2006), 9, pp. 1658-1666, DOI No. 10.1016/j.ijheatmasstransfer.2005.09.039
- [11] Li, Q., *et al.*, Thermal Boundary Resistances of Carbon Nanotubes in Contact with Metals and Polymers, *Nano Letters*, 9. (2009), 11, p. 3805, DOI No. 10.1021/nl901988t
- [12] Hirotsu, J., *et al.*, Experimental Study on Interfacial Thermal Resistance between Carbon Nanotube and Solid Material (Thermal Engineering), *Transactions of the Japan Society of Mechanical Engineers B*, 76. (2010), pp. 1412-1419, DOI No. 10.1299/kikaib.76.769\_1412
- [13] Kong, Q.Y., *et al.*, Novel Three-dimensional Carbon Nanotube Networks as High Performance Thermal Interface Materials, *Carbon*, 132. (2018), pp. 359-369, DOI No. 10.1016/j.carbon.2018.02.052

- [14] Kaur, S., *et al.*, Enhanced Thermal Transport at Covalently Functionalized Carbon Nanotube Array Interfaces, *Nature Communications*, 5. (2014), 2, pp. 1661-1667, DOI No. 10.1038/ncomms4082
- [15] Sun, S., *et al.*, Improving Thermal Transport at Carbon Hybrid Interfaces by Covalent Bonds, *Advanced Materials Interfaces*, 1800318. (2018), pp. 1-9, DOI No. 10.1002/admi.201800318
- [16] Hu, G.J., B.Y. Cao, Thermal Resistance Between Crossed Carbon Nanotubes: Molecular Dynamics Simulations and Analytical Modeling, *Journal of Applied Physics*, 114. (2013), 22, p. 96, DOI No. 10.1063/1.4842896
- [17] Yovanovich, M.M., Four Decades of Research on Thermal Contact, Gap, and Joint Resistance in Microelectronics, *Transactions on Components & Packaging Technologies*, 28. (2005), 2, pp. 182-206, DOI No. 10.1109/TCAPT.2005.848483
- [18] Leung, M., *et al.*, Prediction of Thermal Contact Conductance in Vacuum by Statistical Mechanics, *Journal of Heat Transfer*, 120. (1998), 1, pp. 51-57, DOI No. 10.1115/1.2830064
- [19] Ying, J., *et al.*, Theoretical and Experimental Research on the Contact Thermal Resistance between Real Surface, *Journal of Zhenjiang University (Mechanical Engineering)*, 1. (1997), 1, pp. 104-109
- [20] Xin, H., *et al.*, Buckling and Axially Compressive Properties of Perfect and Defective Single-walled Carbon Nanotubes, *Carbon*, 45. (2007), 13, pp. 2486-2495, DOI No. 10.1016/j.carbon.2007.08.037
- [21] Mesarovic, S.D., *et al.*, Mechanical Behavior of a Carbon Nanotube Turf, *Scripta Materialia*, 56. (2007), 2, pp. 157-160, DOI No. 10.1016/j.scriptamat.2006.09.021
- [22] Liu, Y.Z., *Nonlinear Mechanics of Thin Elastic Rod*. 2006, Tsinghua University Press: Beijing.
- [23] Bahrami, M., *et al.*, Thermal Contact Resistance of Nonconforming Rough Surfaces, Part 1: Contact Mechanics Model, *Journal of Thermophysics and Heat Transfer*, 18. (2004), 2, pp. 218-227, DOI No. 10.2514/1.2661
- [24] Bahrami, M., *et al.*, Thermal Contact Resistance of Nonconforming Rough Surfaces, Part 2: Thermal Model, *Journal of Thermophysics and Heat Transfer*, 18. (2004), 2, pp. 218-227, DOI No. 10.2514/1.2664
- [25] Greenwood, J.A., J.P. Williamson. *Contact of Nominally Flat Surfaces*, Proceedings of the Royal Society of London A: Mathematical, Physical and Engineering Sciences, 1966, 295, pp. 300-319
- [26] Chang, W.R., *et al.*, An Elastic-Plastic Model for the Contact of Rough Surfaces, *Journal of Tribology*, 109. (1987), 2, pp. 257-263, DOI No. 10.1115/1.3261348
- [27] Huang, H., X. Xu, Effects of Surface Morphology on Thermal Contact Resistance, *Thermal Science*, 15. (2011), 5, pp. 33-38
- [28] Kang, J.W., H.J. Hwang, An Ultrathin Carbon Nanoribbon Study as a Component of Nanoelectromechanical Devices, *Molecular Simulation*, 31. (2005), 8, pp. 561-565, DOI No. 10.1080/08927020500044954
- [29] Kang, J.W., *et al.*, Molecular Dynamics Study of Hypothetical Silicon Nanotubes Using the Tersoff Potential, *Journal of Nanoscience & Nanotechnology*, 2. (2002), 6, p. 687, DOI No. 10.1166/jnn.2002.146
- [30] Saidi, P., *et al.*, An Embedded Atom Method Interatomic Potential for the Zirconium-iron System, *Computational Materials Science*, 133. (2017), pp. 6-13, DOI No. 10.1016/j.commatsci.2017.02.028
- [31] Eich, S.M., G. Schmitz, Embedded-atom Study of Low-energy Equilibrium Triple Junction Structures and Energies, *Acta Materialia*, 109. (2016), pp. 364-374, DOI No. 10.1016/j.actamat.2016.02.058
- [32] Mahdavi, M.H., *et al.*, Nonlinear Vibration of a Single-walled Carbon Nanotube Embedded in a Polymer Matrix Aroused by Interfacial Van Der Waals Forces, *Journal of Applied Physics*, 106. (2009), 11, p. 56, DOI No. 10.1063/1.3266174
- [33] Fuller, J.J., E.E. Marotta, Thermal Contact Conductance of Metal/Polymer Joints: An Analytical and Experimental Investigation, *Journal of Thermophysics and Heat Transfer*, 15. (2001), 2, pp. 228-238, DOI No. 10.2514/2.6598
- [34] Cooper, M.G., *et al.*, Thermal Contact Conductance, *International Journal of heat and mass transfer*, 12. (1969), 3, pp. 279-300, DOI No. 10.1016/0017-9310(69)90011-8
- [35] Eric, P., *et al.*, Thermal Conductance of an Individual Single-Wall Carbon Nanotube above Room Temperature, *Nano Letters*, 6. (2006), 1, pp. 96-100, DOI No. 10.1021/nl052145f
- [36] Fujii, M., *et al.*, Measuring the Thermal Conductivity of a Single Carbon Nanotube, *Physical Review Letters*, 95. (2005), 6, p. 065502, DOI No. 10.1103/PhysRevLett.95.065502
- [37] Bi, K.D., *et al.*, Molecular Dynamics Simulation of Thermal Conductivity of Single-wall Carbon Nanotubes, *Physica Letters A*, 350. (2006), 1, pp. 150-153, DOI No. 10.1016/j.physleta.2005.09.070
- [38] Xu, J., T.S. Fisher, Enhanced Thermal Contact Conductance Using Carbon Nanotube Array Interfaces, *Transactions on Components & Packaging Technologies*, 29. (2006), 2, pp. 261-267